6th European Conference on Computational Mechanics (ECCM 6)
7th European Conference on Computational Fluid Dynamics (ECFD 7)
11 – 15 June 2018, Glasgow, UK

Elastoplastic and Nonlinear Analysis of Functionally Graded Axisymmetric Plate-Shell Structures

José S. Moita[1], **Aurélio L. Araújo**[2], **Cristóvão M. Mota Soares**[3], **Carlos A Mota Soares**[4]

[1] IDMEC, Instituto Superior Técnico, Universidade de Lisboa
Av. Rovisco Pais,1 - 1049-001, Lisboa, Portugal
jmoita50@gmail.com

[2] IDMEC, Instituto Superior Técnico, Universidade de Lisboa
Av. Rovisco Pais,1 - 1049-001, Lisboa, Portugal
aurelio.araujo@tecnico.ulisboa.pt

[3]IDMEC, InstitutoSuperiorTécnico, Universidade de Lisboa
Av. Rovisco Pais,1 - 1049-001, Lisboa, Portugal
cristovao.mota.soares@tecnico.ulisboa.pt

[4]IDMEC, InstitutoSuperiorTécnico, Universidade de Lisboa
Av. Rovisco Pais,1 - 1049-001, Lisboa, Portugal
carlos.mota.soares@tecnico.ulisboa.pt

Key Words: *Functionally Graded Materials, Elastoplasticity, Nonlinear Analysis, FEM.*

1 INTRODUCTION

Typical Functionally Graded Material (FGM) plate structures are characterized by a continuous variation of the material properties over the thickness direction by mixing two different materials, metal and ceramic. Ceramic with the low thermal conductivity can resist high thermal environment while metal is strong with mechanical load. The metal–ceramic FGM plates are widely used in aircraft, space vehicles, reactor vessels, and other engineering applications.

Research works in FGM structures has been done in the recent years. For axisymmetric plates and shells, we cite among others, the following works: Reddy et al. [1] study the axisymmetric bending of through the thickness functionally graded circular plates using the Mindlin plate theory. Ma et al. [2] analyse the axisymmetric nonlinear bending behaviour of functionally graded circular plates, under mechanical and thermal loading. Gunes and Reddy [3] present the geometrically nonlinear analysis of functionally graded circular plates. Li et al. [4] study by the stress function method the problem of transversely isotropic functionally graded materials plates. Tran et al. [5] present a NURBS-based isogeometric approach for static, dynamic and buckling analysis of the FGM plates using HSDT model. Zhang and Zhou [6] presented a model for FGM circular plates based on a physical neutral surface and a higher-order shear deformation theory.

Elastoplasticity analysis has been little investigated in FGM structures. Most of the published works involves plate/shells structures made of isotropic materials. In this paper is presented the

static bending analysis of functionally graded of axisymmetric plate-shell type structures subjected to axisymmetric loading. The formulation includes the global response of the plate-shell structures, the through-thickness stress distribution calculations, involving variation of volume fractions. The solutions are obtained using a finite element model based on the Zienckiewics et al. [7] conical frustum simple finite element with 2 nodes, and 3 degrees of freedom per node. The solutions of some illustrative plate examples are performed, and the results are presented, discussed, and compared with numerical alternative models when available.

2 FORMULATION OF P-FGM MODEL

An FGM is made by mixing two distinct isotropic material phases, for example a ceramic and a metal. In this work the material properties of an FGM plate structure is assumed to change continuously throughout the thickness, according to the volume fraction of the constituent materials, given by the Power-Law function – Bao and Wang [8]. In addition, the continuous variation of the materials mixture is approximated by using a certain number of virtual layers k throughout the thickness direction - layer approach. The volume fraction of the ceramic and metal phases for each virtual layer is defined according to the power-law, Moita et al. [9]:

$$V_c^k = \left(0.5 + \frac{\bar{z}}{h}\right)^p \quad ; \quad V_m^k = 1.0 - V_c^k \tag{1}$$

where $\bar{z}$ is the thickness coordinate of mid-surface of each layer.

Once the volume fraction V_c^k and V_m^k have been defined, the material properties, as for example Young's modulus E or thermal expansion coefficient α of each layer of an FGM can be determined by the rule of mixtures:

$$E_k = V_c^k\, E_c + V_m^k\, E_m \quad ; \quad \alpha_k = V_c^k\, \alpha_c + V_m^k\, \alpha_m \tag{2}$$

3 STRAIN-DISPLACEMENT RELATIONS.

A typical axisymmetric shell is shown in Figure 1. For this type of shells, subjected to axisymmetric loading, the displacement of a point on middle surface of meridian plane, is

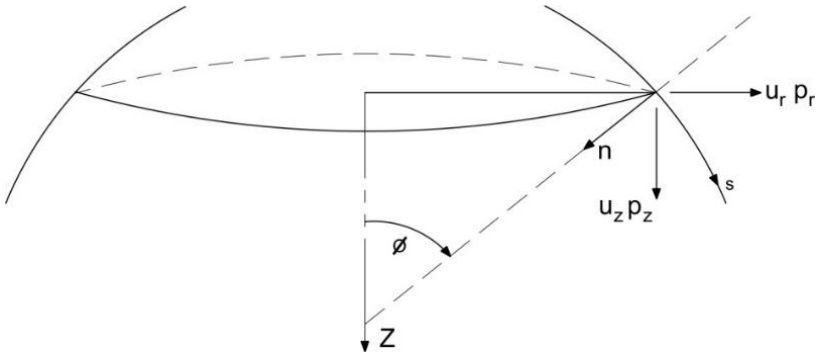

Figure 1. Axisymmetric shell.

determined by two components u_s and w in the tangential (s) and normal (n) directions, respectively. It because, for these conditions $u_\theta = 0$ and $d/d\theta = 0$.

As we are considering a straight finite element, $R = \infty$, from the Kirchhoff type strain, and imposing a constraint $C(w,\beta) = dw/ds - \beta = 0$, introducing the shear strain γ defined as $\gamma = dw/ds - \beta$, the linear strain components in the local curvilinear system are those given in Zienkiewics et al. [7].

3.1 Local-global transformations.

For axisymmetric shells, Figure 1, the relations between local (s,n) and global (r,z) coordinates as well as local-global displacements are given by:

$$\begin{Bmatrix} s \\ n \end{Bmatrix} = \begin{bmatrix} \cos\phi & \sin\phi \\ -\sin\phi & \cos\phi \end{bmatrix} \begin{Bmatrix} r \\ z \end{Bmatrix} \quad ; \quad \begin{Bmatrix} u \\ w \end{Bmatrix} = \begin{bmatrix} \cos\phi & \sin\phi \\ -\sin\phi & \cos\phi \end{bmatrix} \begin{Bmatrix} u_r \\ u_z \end{Bmatrix} \tag{3}$$

For strain-displacements relations, comes:

$$\boldsymbol{\varepsilon} = \begin{Bmatrix} \varepsilon^m \\ \varepsilon^b \\ \varepsilon^s \end{Bmatrix} \begin{Bmatrix} \varepsilon_s \\ \varepsilon_\theta \\ \kappa_s \\ \kappa_\theta \\ \gamma_{sn} \end{Bmatrix} = \begin{Bmatrix} (\partial u_r/\partial s)\cos\varphi + (\partial u_z/ds)\sin\varphi \\ u_r/r \\ -d\beta_r/ds \\ -(\beta_r\cos\varphi)/r \\ -du_r/ds)\ \sin\ \varphi + (du_z/ds)\ \cos\ \varphi - \beta \end{Bmatrix} \tag{4}$$

3.2 Stress-Strain Relations and Constitutive Relations of FGM Structures.

The stress-strain relations for each virtual layer k, can be written as $\sigma_k = \mathbf{Q}_k\ \varepsilon_k$

$$\sigma_k = \begin{Bmatrix} \sigma_s^m \\ \sigma_\theta^m \\ \sigma_s^b \\ \sigma_\theta^b \\ \tau_{sn} \end{Bmatrix} = \begin{bmatrix} Q_{1_k} & 0 & 0 \\ 0 & Q_{1_k} & 0 \\ 0 & 0 & Q_{2_k} \end{bmatrix} \begin{Bmatrix} \varepsilon_s \\ \varepsilon_\theta \\ \bar{z}_k\ \kappa_s \\ \bar{z}_k\ \kappa_\theta \\ \gamma_{sn} \end{Bmatrix} ;\ Q_{1_k} = \begin{bmatrix} \dfrac{E_k}{1-\nu^2} & \dfrac{\nu E_k}{1-\nu^2} \\ \dfrac{\nu E_k}{1-\nu^2} & \dfrac{E_k}{1-\nu^2} \end{bmatrix} ;\ Q_{2_k} = \frac{5}{6}\frac{E_k}{2(1+\nu_k)} \tag{5}$$

where $\mathbf{Q}_k$ is the elasticity matrix. Due to nonsymmetrical grading of the material through the thickness, the bending-stretching coupling exists.The constitutive equation is then given by:

$$\hat{\boldsymbol{\sigma}} = \hat{\mathbf{D}}\ \boldsymbol{\varepsilon} \quad ; \quad \begin{Bmatrix} N \\ M \\ Q \end{Bmatrix} = \begin{bmatrix} A & B & 0 \\ B & D & 0 \\ 0 & 0 & A_s \end{bmatrix} \begin{Bmatrix} \varepsilon^m \\ \varepsilon^b \\ \varepsilon^s \end{Bmatrix} \tag{6}$$

where $\hat{\boldsymbol{\sigma}}$ are the resultant forces and moments, and $\hat{\mathbf{D}}$ the constitutive matrix.

4 ELASTO-PLASTIC FORMULATION FOR FGM STRUCTURES

The present work uses an extended Tamura–Tomota–Ozawa (TTO) model to describe the elastic–plastic behaviour of ceramic/metal FGM. The ceramic constituent is assumed elastic when deformation takes place. The elastoplastic deformation occurs mainly by the plastic flowing of the metallic constituent. The TTO model, or also called the modified rule-of-mixture, uses the stress-strain transfer parameter q, which depends on the constituent material properties and the microstructural interaction in the FG material, [10]. Using this parameter, the thickness variation of Young's modulus and of the yield stress are obtained [10]:

$$E^k = \left(V_m E_m \frac{q+E_c}{q+E_m} + V_c E_c \right) \Bigg/ \left(V_m \frac{q+E_m}{q+E_c} + V_c \right)$$

$$\sigma_Y^k = \sigma_{Ym} \left(V_m^k + \frac{q+E_m}{q+E_c} \frac{E_c}{E_m} V_c^k \right) \tag{7}$$

4.1 Elastoplastic constitutive relation

To carry out elastoplastic analysis, the material is assumed to follows the von-Mises yielding criterion. The yield condition can be expressed as, Nayak and Zienckiewics [11]:

$$F\left(\sigma,\ \varepsilon_p,\ \kappa\right) = f\left(\sigma\right) - \sigma_Y\left(\kappa\right) = 0 \tag{8}$$

where ε_p is the accumulated plastic strain, and where the yield level, σ_Y, can be a function of the strain hardening parameter κ.

For the case of an isotropic material, and for each layer of a FGM structure, the effective stress $\overline{\sigma}$, is given by:

$$f(\sigma) = \overline{\sigma}_k = \left[\sigma_{s_k}^2 + \sigma_{\theta_k}^2 - \sigma_{s_k}\sigma_{\theta_k} + 3\,\tau_{sn_k}^2 \right]^{1/2} \tag{9}$$

After development, an incremental constitutive elastoplastic relation is given by [11]:

$$d\boldsymbol{\sigma}_k = \mathbf{Q}_k^{ep}\, d\boldsymbol{\varepsilon} \quad ; \quad \mathbf{Q}_k^{ep} = \mathbf{Q}_k - \frac{\mathbf{Q}_k\, \mathbf{a}\, \mathbf{a}^T \mathbf{Q}_k}{A + \mathbf{a}^T \mathbf{Q}_k\, \mathbf{a}} \tag{10}$$

where $\mathbf{Q}^{ep}$ is the elastoplastic matrix, and $\mathbf{a} = dF/d\sigma$ is the flow vector.

5 FINITE ELEMENT APROACH.

In the present work is used a conical frustum – straight finite element, Figure 4, with two nodes and three degrees of freedom per node, the displacements and rotation, $u_{ri}, u_{zi}\ \beta_i$. The simplest interpolation is given by Zienkiewics et al. [7]:

$$N_i = (1 + \xi_i \xi)/2 \tag{11}$$

for an element with nodes at $\xi_i = \mp 1$, with $\xi_i = 2\,s_i / L$, $s_i = \mp L/2$

The nodal displacement vector, is then given by:

$$\begin{Bmatrix} u_r \\ u_z \\ \beta \end{Bmatrix} = \sum_{i=1}^{2} \begin{bmatrix} N_i & 0 & 0 \\ 0 & N_i & 0 \\ 0 & 0 & N_i \end{bmatrix} \begin{Bmatrix} u_{ri} \\ u_{z_i} \\ \beta_i \end{Bmatrix} \; ; \; \mathbf{u=N\,a} \tag{12}$$

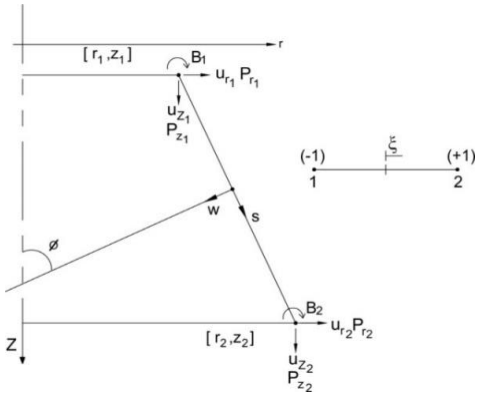

Figure 4. Conical frustum element

The linear strains can be represented by: $\boldsymbol{\varepsilon} = \mathbf{B}\,\mathbf{a}$; $\boldsymbol{\varepsilon} = \sum_{i=1}^{2} \mathbf{B_i}\,\mathbf{d}_i$, where $\mathbf{B}_i$ is given by:

$$\mathbf{B}_i = \begin{bmatrix} \frac{dN_i}{ds}\cos\phi & \frac{dN_i}{ds}\sin\phi & 0 \\ \frac{N_i}{r} & 0 & 0 \\ 0 & 0 & -\frac{dN_i}{ds} \\ 0 & 0 & -N_i\frac{\cos\phi}{r} \\ -\frac{dN_i}{ds}\sin\phi & \frac{dN_i}{ds}\cos\phi & -N_i \end{bmatrix} \; ; \quad \frac{dN_i}{ds} = \frac{dN_i}{d\xi}\frac{d\xi}{ds} = \frac{\xi_i}{L} \tag{13}$$

Accounting for nonlinear response, nonlinear strains have to be considered. For this type of structures the nonlinear strain, in local system is $\varepsilon^{NL} = (1/2)(dw/ds)^2$, which is expressed as

$$\boldsymbol{\varepsilon}^{NL} = \frac{1}{2}\mathbf{a}^T\,\mathbf{G}^T\,\mathbf{G}\,\mathbf{a} \tag{14}$$

where $\mathbf{G}_i$ is given by:

$$\mathbf{G} = \sum_{i=1}^{2} \begin{bmatrix} -\frac{dN_i}{ds}\sin\phi & 0 & 0 \\ 0 & \frac{dN_i}{ds}\cos\phi & 0 \end{bmatrix} \tag{15}$$

5.1 Elastoplastic analysis

The virtual work principle applied to elastoplastic analysis is given by:

$$\sum_{k=1}^{N}\left\{\int_{A^e}\int_{h_{k-1}}^{k_k}\delta\boldsymbol{\varepsilon}_k^L\ \mathbf{Q}_k^{ep}\ \boldsymbol{\varepsilon}_k^L\ dz\,dA^e\right\}=\delta\ \mathbf{a}^T\mathbf{F}_{ext}^e-\sum_{k=1}^{N}\int_{A^e}\int_{h_{k-1}}^{k_k}\delta\boldsymbol{\varepsilon}_k^L\ \sigma_k^L\ dz\,dA^e \tag{16}$$

Entering with the previous definitions, and integrating through the thickness, Equation (16) can be written in the following form:

$$\int_{A^e}\delta\mathbf{a}^T\mathbf{B}^T\hat{\mathbf{D}}^{ep}\,\mathbf{B}\,\Delta\mathbf{a}\,dA^e=\delta\ \mathbf{a}^T\mathbf{F}_{ext}^e-\delta\ \mathbf{a}^T\mathbf{F}_{int}^e\ ;\ \int_{A^e}\mathbf{B}^T\hat{\mathbf{D}}^{ep}\mathbf{B}\,\Delta\mathbf{a}\,dA^e=\mathbf{F}_{ext}^e-\mathbf{F}_{int}^e \tag{17}$$

5.2 Geometrically nonlinear analysis

The virtual work principle in conjugation with an updated Lagrangian formulation is used, where a reference configuration is associated with a previous time t and the actualized configuration is associated with the current time $t+\Delta t$. The linearized equilibrium equations for nonlinear static response, written for a finite element, are given by, Bathe [12]

$$\int_{^tA^e}\delta\mathbf{a}^T\mathbf{B}^T\hat{\mathbf{D}}\mathbf{B}\,\Delta\mathbf{a}\ {}^tdA^e+\int_{^tA^e}\delta\mathbf{a}^T\mathbf{G}\ {}^t\hat{\sigma}\ \mathbf{G}\,\Delta\mathbf{a}\ {}^tdA^e=\delta\ \mathbf{a}^T\mathbf{F}_{ext}^e-\delta\ \mathbf{a}^T\mathbf{F}_{int}^e$$

$$\int_{^tA^e}\mathbf{B}^T\hat{\mathbf{D}}\mathbf{B}\,\Delta\mathbf{a}\ {}^tdA^e+\int_{^tA^e}\mathbf{G}\ {}^t\hat{\sigma}\ \mathbf{G}\,\Delta\mathbf{a}\ {}^tdA^e=\mathbf{F}_{ext}^e-\mathbf{F}_{int}^e \tag{18}$$

where the linear and geometric stiffness matrices, external force vector (including distributed and concentrated transverse loads **f** and $\mathbf{F}_c$, as well as in-plane load **t**), and internal force vector are given by:

$$\mathbf{K}_L^e=\int_{^tA^e}\mathbf{B}^T\ \hat{\mathbf{D}}\ \mathbf{B}\ {}^tdA^e\ ;\ \mathbf{K}_\sigma^e=\int_{^tA^e}\mathbf{G}^T\ {}^t\bar{\boldsymbol{\sigma}}\ \mathbf{G}\ {}^tdA^e$$

$$\mathbf{F}_{ext}^e=\int_{^0A^e}\mathbf{N}^T\mathbf{f}\ \ {}^0dA^e+\mathbf{F}_c\ ;\ \mathbf{F}_{int}^e=\int_{^tA^e}\mathbf{B}^T\ {}^t\hat{\boldsymbol{\sigma}}\ \ {}^tdA^e\ ;\ {}^t\bar{\boldsymbol{\sigma}}=\begin{bmatrix}{}^t\mathbf{N}_s & 0\\ 0 & {}^t\mathbf{N}_s\end{bmatrix} \tag{19}$$

and where ${}^tdA^e=2\,\pi\ {}^tr\ {}^tds=\pi\ {}^tr\ {}^tL\,d\xi$.

6 APPLICATIONS

6.1 Linear analysis of circular FGM plate under pressure load.

In this section, the behaviour of a FGM clamped circular plate, Figure 5, with thickness h and radius R made of titanium/zirconium is studied (E_m = 110.25 GPa, ν_m=0.288, E_c = 278.41GPa, ν_c= 0.288). Based on the rule of mixture, the effective modulus is estimated following Reddy et al. [1]: $E(z)=(E_m-E_c)\ V_m+E_c$ with $V_m^k=\left(0.5-\bar{z}/h\right)^p$; $V_c^k=1-V_m^k$.

This equation shows that as p = 0, the plate is fully metal and as p=∞, the plate is fully ceramic. Under uniform pressure, the normalized maximum deflections (at the centre of the plate) are given by $\bar{w}_c = w_c\ (64\ D_c\ /\ q\ R^4)$, $D_c = E_c h^3/12(1-\nu^2)$, and shown in Table 1. An excellent agreement is observed between the results obtained with the present model and the results obtained using Mindlin theory [1], elasticity theory [4] and HSDT theory [5]. The deformed shapes under transverse pressure load ($q_0 = 1.0\,\mathrm{MPa}$) for different gradient index and h/R=0.05, are shown in Figure 6. As expected the full metal and ceramic plates ate the maximum and minimum deflections according to the respective Young modulus. Also the through-thickness distribution of nondimensional radial stress is presented in Figure 7. A comparison with the solution obtained by Li et al. [4] reveals to be very good.

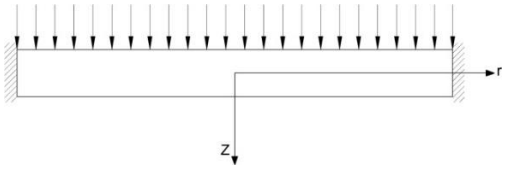

Figure 5. Clamped circular plate, subjected to a uniform load

Table 1. Dimensionless central deflection $\overline{w}_c$ of FGM clamped circular plate.

h/R	Source	Power index p						
		0	2	4	10	50	100	metal
0.05	Li[4]	2.561	1.405	1.284	1.157	1.049	1.032	1.015
	Reddy[1]	2.554	1.402	1.282	1.155	1.046	1.029	1.011
	Tran[5]	2.548	1.399	1.279	1.152	1.044	1.027	1.009
	PM	2.560	1.404	1.283	1.155	1.043	1.024	1.015
0.1	Li[4]	2.667	1.456	1.329	1.201	1.091	1.074	1.057
	Reddy[1]	2.639	1.444	1.320	1.190	1.080	1.063	1.045
	Tran[5]	2.630	1.439	1.314	1.186	1.076	1.059	1.042
	PM	2.643	1.446	1.321	1.189	1.076	1.058	1.046

6.2 Nonlinear Analyses of Circular FGM Plate under Uniform Pressure Load.

A clamped P-FGM circular plate with radius-to-thickness ratios R/h=20 is considered. The constituents of the FGM are the Si_3N_4 and SUS304 with the following materials properties E_c=322.27 GPa, E_m = 207.79 GPa, ν_c =0.24, ν_m = 0.318, and the volume fraction is defined by $V_c = (0.5 - \bar{z}/h)^p$. The radius of circular plate is R=0.5 m, and the thickness is h=0.025 m. A geometrically nonlinear analysis (GNL) under uniform pressure load at room temperature (300 K) is performed. The plate is modelled by 20 finite elements (66 DOFs). Defining the nondimensional loads and displacements respectively by $Q = q_0\ R^4 / E_m h^4$ and w_c/h, the load-displacement paths for centre point of the plate obtained using the present model are shown in Figure 8 for different gradient p-index. A very good agreement with the results obtained by Zhang and Zhou [6] is observed.

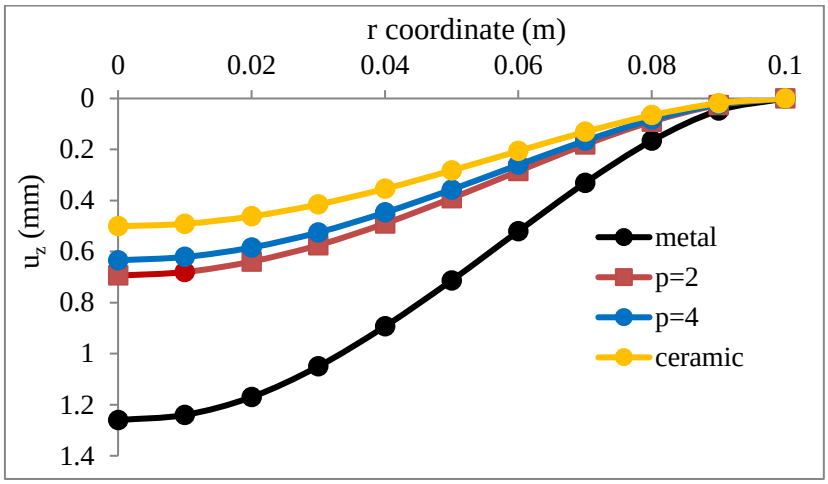

Figure 6. Deflection shapes of a clamped circular FGM plate for different p-index

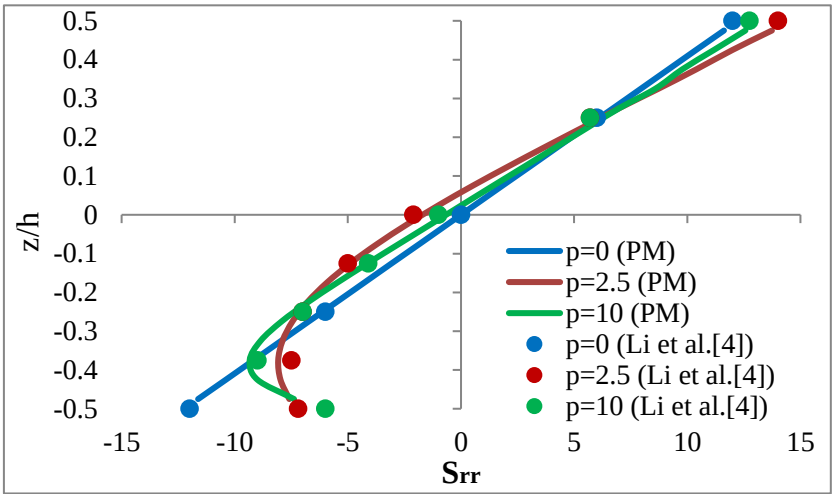

Figure 7. Through-thickness distribution of nondimensional stress for different p-index

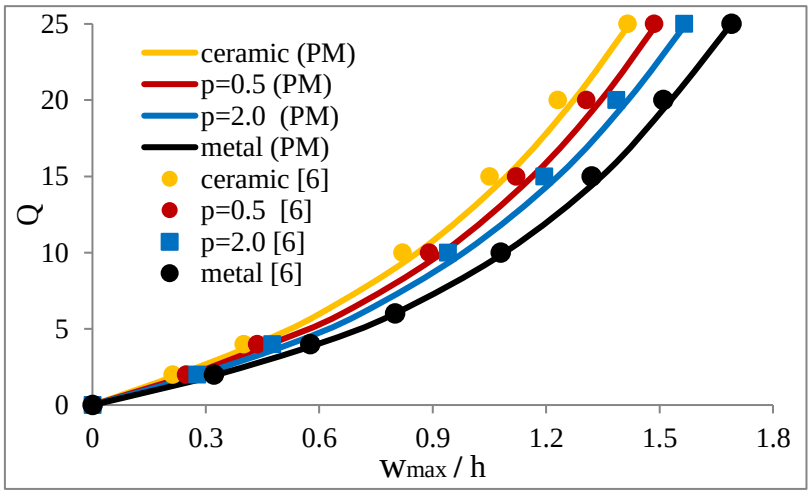

Figure 8. Nonlinear load-displacement paths of a clamped FGM pate.

Next, considering the same plate, an elastoplastic analysis (EPL) with $\sigma_{Ym} = 400$ MPa is also performed. In Figure 9 are present the results obtained using the present model. From Figures 8 and 9 we observe a very significant difference between the maximum loads allowed considering the elastoplastic and the geometrically nonlinear behaviours. Thus, for real structures, the combination of these two behaviours should be considered to obtain the realistic response of the structures. This response for the present application is shown in Figure 10.

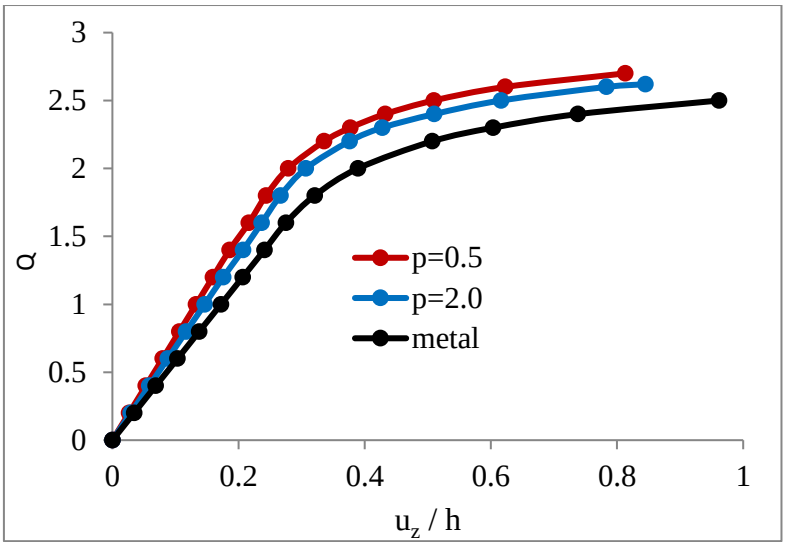

Figure 9. Load-displacement paths in elastoplasticity for a clamped FGM plate.

6.3 Nonlinear analysis of a pressure vessel with torispherical end

The static deformation of a FGM cylindrical pressure vessel with torispherical end is analysed. This structure is represented in Figure 11, where $R=D_i=135$ mm, $t=1.27$ mm, $r_1=10.1$ mm, and is made of constituents zirconia and aluminum ($E_m = 68.9476$ GPa, $\nu_m = 0.3$, $\sigma_Y = 247$ MPa, $E_c = 151.0$ GPa, $\nu_c = 0.3$), and is subjected to an inner pressure load $p_0=1$ MPa. The u_z displacement at the apex for different p-index are present in Table 2. The elastoplastic analysis is also performed. Using the present model the collapse pressures as a function of p-index are also given in Table 2. The deformed shapes (enlarged 20 times) for metal and gradient index p=0.5 are shown in Figure 12. The deformed shape in elastoplastic behaviour for metal (enlarged 10 times), for limit uniform pressure of 2.6 MPa, is also shown in Figure 12, with the plastic zone in yellow. In Figure 13 are shown the elastoplastic load-displacement paths for metal and gradient index p=0.5.

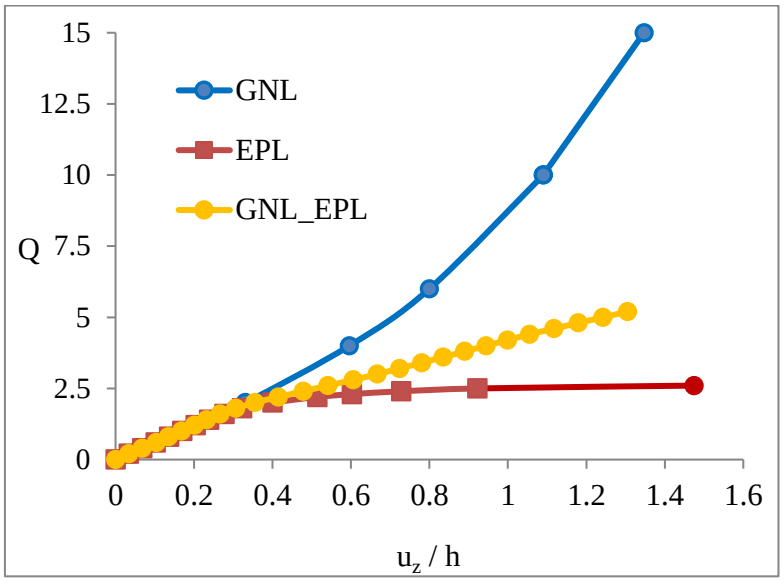

Figure 10. Load-displacement paths for different behaviours of a FGM circular plate

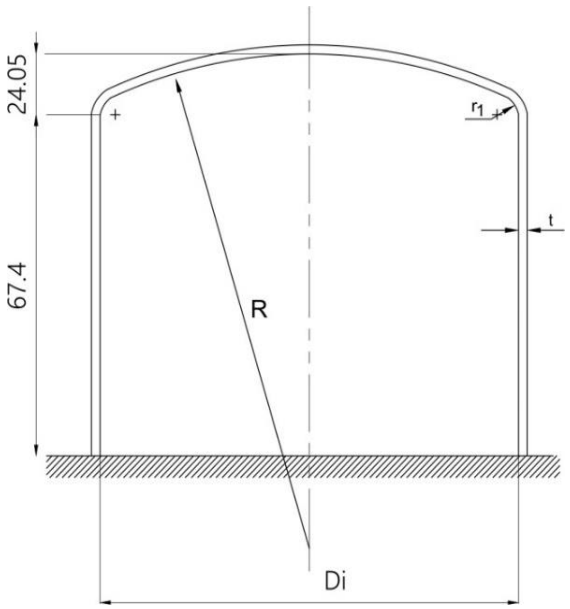

Figure 11. Pressure vessel

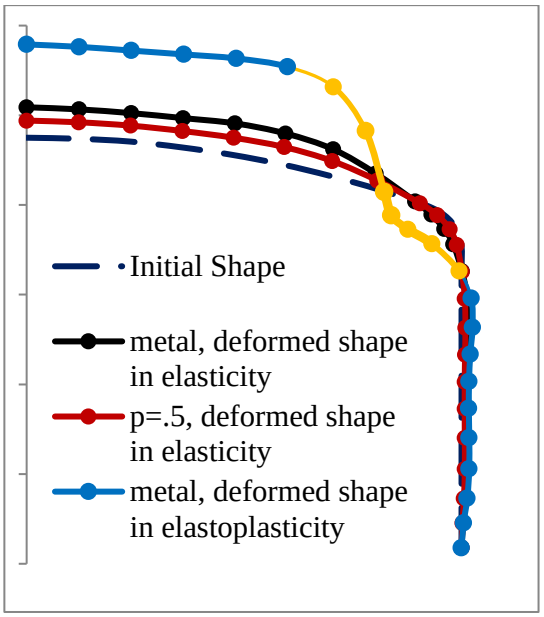

Figure 12. Deformed shapes of the pressure vessel

Table 2. Displacement (mm) for p=1.0 MPa, and collapse pressure in FGM pressure vessel with torispherical ends

	p-index			
	0.5	1.0	2.0	metal
Deflection u_z	0.189	0.213	0.241	0.337
Collapse p	3.46	3.36	3.25	2.60

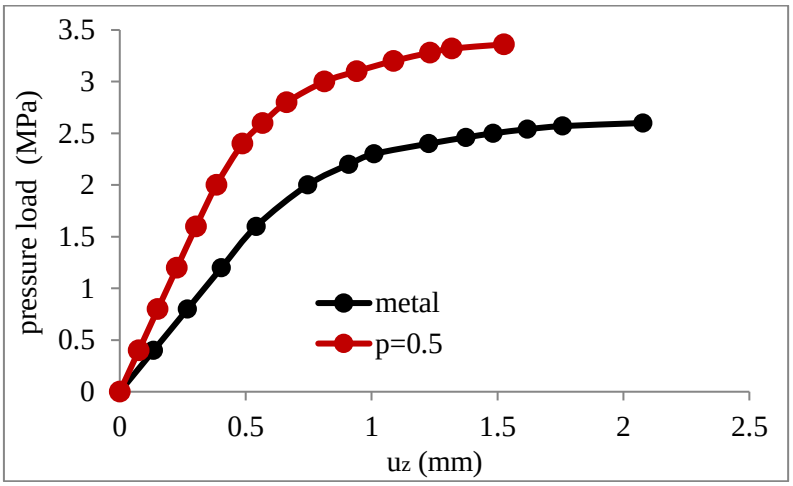

Figure 13. . Load-displacement paths in elastoplasticity for the FGM pressure vessel.

The responses for the present application, considering the metal phase, with different mechanical behaviours are shown in Figure 14. From this Figure, it is observed that real behaviour (GNL+EPL) gives a limit pressure greater than the limit pressure obtained using a pure elastoplastic analysis.

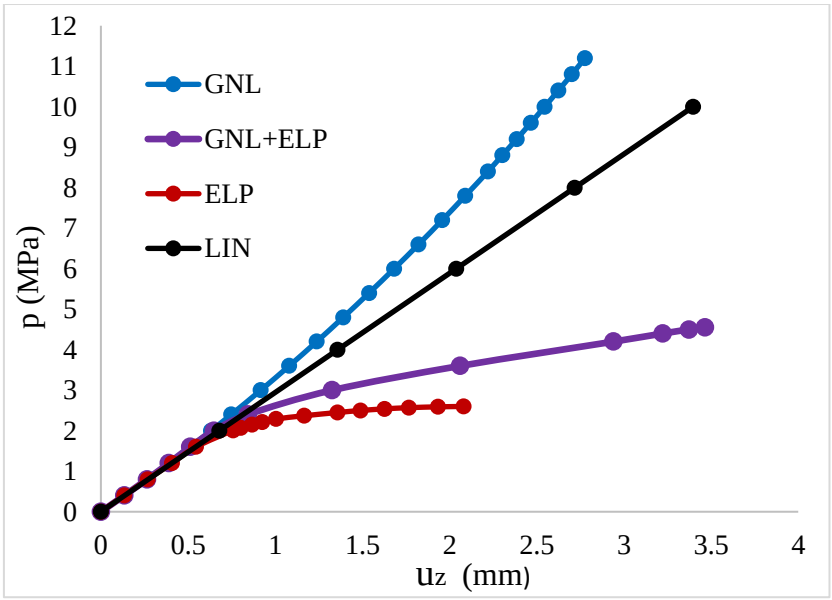

Figure 14. Load-displacement paths for different deformation behaviours of a pressure vessel

7 CONCLUSIONS

- A finite element model for the static bending, buckling and free-vibration analyses of functionally graded (FGM) circular plates and axisymmetric shells under axisymmetric loading is presented. The model is based on the classic plate theory that takes into account shear deformation through a penalty function, associated with a simple and fast conical frusta finite element with only 2 nodes and 3 degrees of freedom per node.

- The reduced number of finite elements necessary to model even complex structures combined with the use of only twenty virtual layers to model the continuous variation of the mechanical properties through the thickness, results in an extremely lower computational time for all FGM applications.
- A good to very good accuracy is found when the results obtained by the present model are compared with solutions available and obtained by alternative models. Some applications are also proposed, which can be used as benchmark test.
- As final conclusion, the present model is a very simple, accurate, and fast finite element model for the analysis of axisymmetric shells under axisymmetric loads.

ACKNOWLEDGEMENTS:

This work was supported by FCT, Fundação para a Ciência e Tecnologia, through IDMEC, under LAETA, project UID/EMS/50022/2013.

REFERENCES

[1] Reddy, J.N., Wang C.M., Kitiporncha, S. Axisymmetric bending of functionally graded circular and annular plates. *Eur. J. Mech. A/Solids* (1999) **18**: 185-199.

[2] Ma, L., Deng, C., Ou, Z. Nonlinear bending of FGM circular plates with temperature-dependent properties. *Materials Science Forum* (2008) **575-578**: 1020-1024.

[3] Gunes, R. and Reddy, J.N. Nonlinear analysis of Functionally Graded circular plates. *International Journal of Structural Stability and Dynamics* (2008) **8** (1): 131–159.

[4] Li, X.Y., Ding, H.J., Chen, W.Q. Elasticity solutions for a transversely isotropic functionally graded circular plate subject to an axisymmetric transverse load qr^k. *International Journal of Solids and Structures* (2008) **45**: 191–210.

[5] Tran, L.V., Ferreira, A.J.M., Nguyen-Xuan, H. Isogeometric analysis of functionally graded plates using higher-order shear deformation theory. *Composites: Part B* (2013).

[6] Zhang D.G., Zhou H.M. Nonlinear bending analysis of FGM circular plates based on physical neutral surface and higher-order shear deformation theory. *Aerospace Science and Technology* (2015), http://dx.doi.org/10.1016/j.ast.2014.12.016.

[7] Zienkiewics, O.C., Bauer, J., Morgan, K., Onate, E. A simple and efficient element for axisymmetric shells. *International Journal for Numerical Methods in Engineering* (1977) **11**: 1545 - 1558.

[8] Bao, G., Wang L. Multiple cracking in functionally graded ceramic/metal coatings. *International Journal of Solids and Structures* (1995) **32**: 2853–2871.

[9] Moita, J.S., Araújo, A.L., Mota Soares, CM., Mota Soares, C.A., Herskovits, J. Material and geometric nonlinear analysis of functionally graded plate-shell type structures. *Applied Composite Materials* (2016) **23** (4): 537–554.

[10] Jin, J.H., Paulino, G.H., Dodds Jr, R.H. Cohesive fracture modeling of elastic–plastic crack growth in functionally graded materials. *Eng Fract Mech.* (2003) **70** (14): 1885–912.

[11] Nayak, G.C, Zienckiewics, O.C. Elastoplastic stress analysis. A generalization for various constitutive relations including strain softening. *International Journal for Numerical Methods in Engineering* (1972) **5**: 113-135.

[12] Bathe K.J., Ho L.W. A simple and effective element for analysis of general shell structures. *Computers and Structures* (1981) **13**: 673-681.